



Second generation of BACE-1 inhibitors. Part 1: The need for improved pharmacokinetics

Nicolas Charrier, Brian Clarke, Leanne Cutler, Emmanuel Demont*, Colin Dingwall, Rachel Dunsdon, Julie Hawkins, Colin Howes, Julia Hubbard, Ishrut Hussain, Graham Maile, Rosalie Matico, Julie Mosley, Alan Naylor, Alistair O'Brien, Sally Redshaw, Paul Rowland, Virginie Soleil, Kathrine J. Smith, Sharon Sweitzer, Pam Theobald, David Vesey, Daryl S. Walter, Gareth Wayne

Neurology and Gastrointestinal Centre of Excellence for Drug Discovery, GlaxoSmithKline R&D, New Frontiers Science Park, Third Avenue, Harlow, Essex CM19 5AW, United Kingdom

ARTICLE INFO

Article history:

Received 25 February 2009

Revised 30 March 2009

Accepted 30 March 2009

Available online 17 April 2009

Keywords:

Alzheimer

BACE-1

Aspartic protease

Hydroxyethylamine

ABSTRACT

Inhibition of the aspartyl protease BACE-1 has the potential to deliver a disease-modifying therapy for Alzheimer's disease. We have recently disclosed a series of transition-state mimetic BACE-1 inhibitors showing nanomolar potency in cell-based assays. Amongst them, GSK188909 (compound **2**) had favorable pharmacokinetics and was the first orally bioavailable inhibitor reported to demonstrate brain amyloid lowering in an animal model. In this Letter, we describe the reasons that led us to favor a second generation of inhibitors for further in vivo studies.

© 2009 Elsevier Ltd. All rights reserved.

Alzheimer's disease (AD) is a devastating neurodegenerative disorder for which no disease-modifying treatment is currently available.¹ It is characterized pathologically by the presence of extracellular senile plaques and intracellular neurofibrillary tangles.² These plaques are mainly comprised of Amyloid- β ($A\beta$) peptides, predominantly of 40 or 42 amino acids in length ($A\beta_{40}$, $A\beta_{42}$), generated by the proteolytic processing of a larger membrane-bound precursor protein, known as the amyloid precursor protein (APP). The identification of BACE-1 (β -site APP cleaving enzyme) as the elusive β -secretase, a key enzyme in the production of $A\beta$ peptides was a major advance in the field of AD.³ Due to the potential for disease modification, many pharmaceutical companies and academic institutions have been actively developing BACE-1 inhibitors for the treatment of AD.⁴

We have recently reported the discovery of a series of novel hydroxyethylamine BACE-1 inhibitors from a micromolar hit **1** (Fig. 1).⁵ Exemplars from this advanced series of inhibitors demonstrated nanomolar potency in cell-based assays and GSK188909 (compound **2**), an example with high potency and favorable in vivo pharmacokinetics was successfully used to demonstrate that inhibiting BACE-1 lowered brain amyloid levels in transgenic mice.⁶ A second generation of inhibitors, typified by compound **3**, demonstrated improved pharmacokinetics whilst retaining the

same high level of potency.^{4c} Herein, and in the following papers, we will present the data that led us to the discovery of these inhibitors and the advantages they offered over earlier compounds.

Inhibitors **4** and **5** (Fig. 2) are further representative of our first generation of inhibitors. As shown in Table 1, the intrinsic properties of these molecules are typical of those reported for marketed renin or HIV protease inhibitors (PIs): high molecular weight (>550), high polar surface area and a high molecular volume (as described by their calculated molar refractivity (CMR) values). These properties are fairly typical of inhibitors of aspartyl proteases that need to make a relatively high number of hydrogen bonding and lipophilic interactions to achieve significant levels of inhibition.

Compound **2** shows high microsomal clearance in all species and also inhibits P450 enzymes at relatively low concentrations (mainly the 3A4 isoforms—as is the case for most of the compounds in this series, Table 1). However, it was possible to minimize this inhibition by lowering the lipophilicity of the inhibitors (compare **5–2** and **4**) but to the detriment of their permeability.

Indeed, although compound **5** was permeable enough to show good activity in a cellular assay,⁷ its oral bioavailability in rats, even at high doses (100 mg/kg) and using an optimized vehicle [suspension in 50% (w/v) Vit E TPGS (*D*- α -tocopheryl polyethylene glycol 1000 succinate), 40% (v/v) PEG 400 and 10% (v/v) ethanol], was poor (0.2%) despite having moderate blood clearance (64 mL/min/kg) suggesting poor absorption. The opposite was observed for the more lipophilic inhibitor **4** (Table 2): this inhibitor

* Corresponding author. Tel.: +44 0 1438764319; fax: +44 0 1438768232.

E-mail address: emmanuel.h.demont@gsk.com (E. Demont).

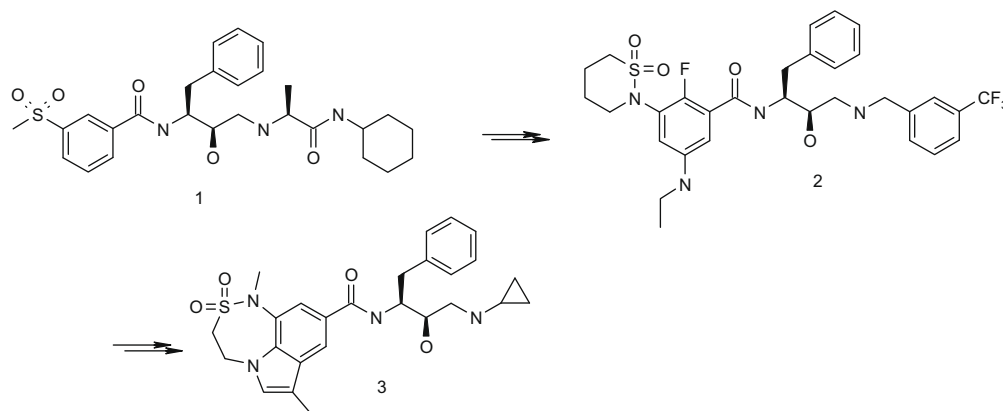


Figure 1. From micromolar hit to nanomolar orally available BACE-1 inhibitors.

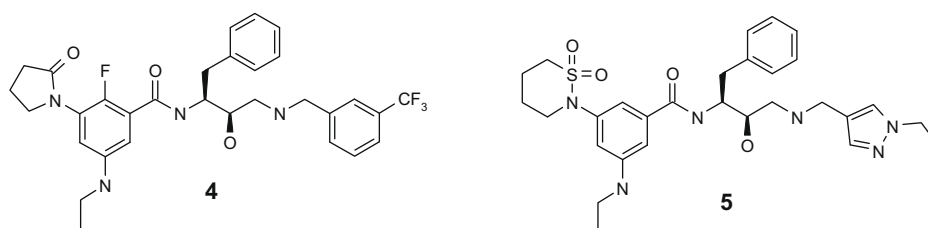


Figure 2. Representative examples of BACE-1 inhibitors.

Table 1

In vitro profile of representative first generation BACE-1 inhibitors

Compd	BACE IC ₅₀ (μM)	Aβ ₄₀ IC ₅₀ (nM)	CYP IC ₅₀ ^b (μM)	Cl ^c (m, r, h)	Log D @ pH 7.4	MW	PSA	CMR
2	0.002	5, 30	>100, 9, 10, 6.2, 0.4, 1.6	37, 8.7, 15	3.29	637	111	16.2
4	0.009	40, 519	75, 60, 15, 11, 75, 6.3	26, 7.6, 14	2.98	587	94	15.3
5	0.010	78, 3633	All >89 (3A4 DEF)	5.4, 1.7, 4.2	0.53	569	129	15.8

^a In SHSY5Y wild type and Swedish cells, respectively. See Ref. 6 for details.

^b 1A2, 2C9, 2C19, 2D6, 3A4 (DEF, PPR).

^c Microsomal clearance in mouse, rat and human, respectively (in ml/min/g liver).

showed similar bioavailability ($\approx 35\%$) following oral administration (3 mg/kg po) or injection via the hepatic portal vein, suggesting complete absorption.

These differences in absorption could be predicted in this series using an in house model based on CMR and lipophilicity (measured

Log D @ pH 7.4). As shown in Figure 3, prediction of absorption for 4 and 5 correlated with in vivo data. Compound 2 had some degree

Table 2

In vivo pharmacokinetics for compounds 2 and 4

Dose route	Parameter	4	2
Intravenous ($n = 3/4$)	CLb ^a (mL/min/kg)	51 ± 9 ^b	83 ± 5 ^d
	Vss (L/kg)	4.5 ± 0.7	5.5 ± 0.6
	$t_{1/2}$ (iv) (h)	1.9 ± 0.3	1.5 ± 0.3
	F _{ipv} (%)	38 ± 11	Nd
Oral @ 3 mg/kg ($n = 4$)	F _{po} (%)	35 ± 15 ^c	Nd
	$t_{1/2}$ (po) (h)	2.1, nd, 1.8, nd	Nd
	AUC/dose (min g/L)	6.9 ± 2.9	Nd
Oral @ 10 mg/kg ($n = 3/4$)	F _{po} (%)	67 ± 45 ^c	7 ± 2 ^e
	$t_{1/2}$ (po) (h)	1.8, 3.1, nd, nd	Nd
	AUC/dose (min kg/L)	17.3 ± 14.8	0.86 ± 0.24

^a CLb: in vivo clearance; Vss: volume of distribution; $t_{1/2}$: half-life; F: bioavailability (following administration in portal vein:ipv or oral administration: po).

^b Dissolve in 2% (v/v) DMSO then added to saline containing 10% (w/v) kleptose.

^c Solution in 5% (v/v) ethanol, Capmul MCM C8 and solutol HS 15 (20:80).

^d 0.9% (w/v) saline containing 10% (w/v) kleptose.

^e Dissolved in 1% (v/v) Tween 80 and 1% (w/v) methylcellulose aqueous. Nd = not determined.

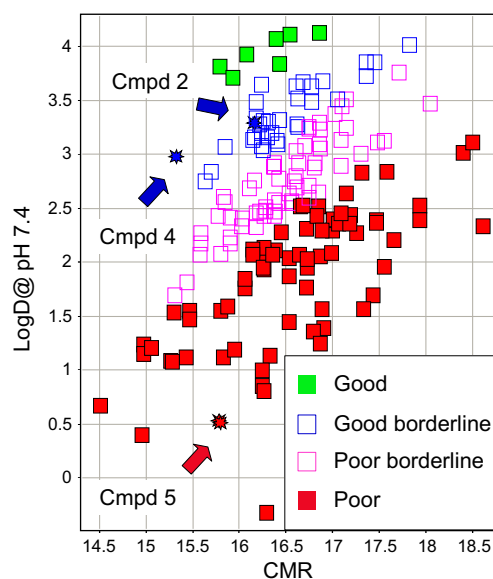


Figure 3. Prediction of absorption for the first generation of inhibitors.

of oral bioavailability despite having high in vivo clearance (Table 2), again suggesting relatively good absorption, in agreement with the prediction.

As can be seen, most of the compounds made in this series were predicted to be poorly absorbed. The compounds which were predicted to be well absorbed were in general too lipophilic to be metabolically stable. Overall, the chemical space available for combining good potency (which tended to correlate with high CMR), good absorption and drug-like lipophilicity was small.

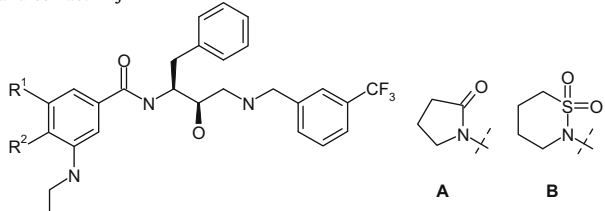
The in vivo profile of inhibitor **4** is similar to what has been reported for HIV PIs: first pass elimination may explain the sub-optimal bioavailability observed after ipv administration and the

non linear kinetics (increased AUC/D between the 10 and 3 mg/kg oral doses) suggest saturation of metabolism at the higher dose.

The oral bioavailability of compound **2** was lower than that of compound **4** but its in vitro activity (especially in cell assays) made it better suited for use as a tool molecule in animal models. Indeed, it proved efficacious in lowering level of amyloid in the brain, albeit at high doses (250 mg/kg po). This molecule, the result of several rounds of optimization, was unlikely to be further optimized in terms of in vitro activity and thus in order to identify a molecule which was efficacious at lower oral doses, the poor pharmacokinetics of our inhibitors had to be optimized further.

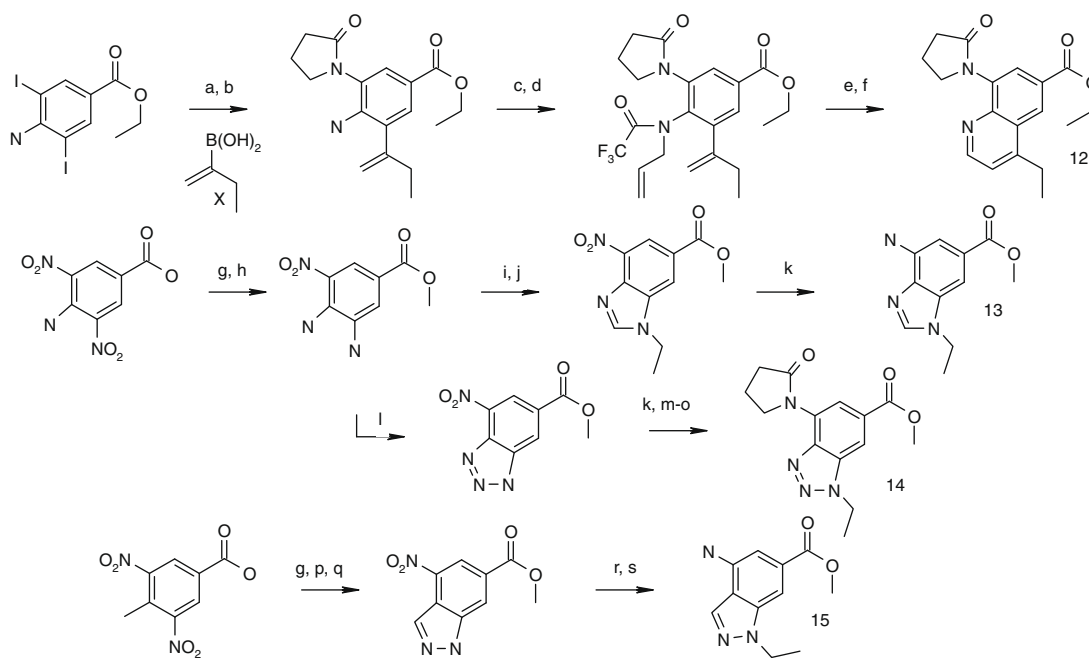
Our strategy towards optimization of the PK properties focused on improving metabolic stability as much as possible in

Table 3
Influence of C-4 substitution to enzyme activity and cell activity



Compd	R ¹	R ²	BACE-1 ^a IC ₅₀ (μM)	BACE-2 IC ₅₀ (μM)	Cat-D IC ₅₀ (μM)
6	A	H	0.049	4.485	6.580
7	A	CH ₃	0.063	9.120	4.270
8	A	OCH ₃	0.110	8.130	3.720
9	B	H	0.005	1.160	3.570
10	B	CH ₃	0.023	7.080	0.980
11	B	OCH ₃	0.018	4.170	0.600

^a In all tables, IC₅₀s reported are means of the values of three different experiments. Each IC₅₀ is within threefold of the mean value.



Scheme 1. Synthesis of key intermediates for the synthesis of biaryl non prime side substituent. Conditions: (a) pyrrolidinone, CuI, K₃PO₄, TMEDA, toluene, reflux 16 h, 28%; (b) X, Pd(PPh₃)₄, K₂CO₃, DME/H₂O 3:1, reflux 6 h, 60%; (c) (CF₃CO)₂O, pyridine, CH₂Cl₂, 25 °C, 61%; (d) allyl bromide, K₂CO₃, acetone, reflux, 3 h, 85%; (e) Grubbs II 10% w/w, CH₂Cl₂, 25 °C, 16 h, 70%; (f) K₂CO₃, EtOH/H₂O 5:1, 25 °C, 2 h then AcOEt, air, 16 h, 79%; (g) MeOH, H₂SO₄, reflux; (h) Pd/C, MeOH/*c*-C₆H₁₂, reflux, 80% (2 steps); (i) EtI, K₂CO₃, DMF, 60 °C, 8 h, 50%; (j) HCOOH, 100 °C, 45 min, 79%; (k) NH₄COOH, Pd/C, MeOH/H₂O, 70 °C, 30 min, 81%; (l) NaNO₂, AcOH, 60 °C, 1 h, 78%; (m) Cl(CH₂)₃COCl, NEt₃, CH₂Cl₂, 25 °C; (n) NaH, THF, 25 °C; (o) NaH, DMF, 25 °C then EtI, 2 h, 61%; (p) Pd/C, MeOH/*c*-C₆H₁₂, reflux, 84% (2 steps); (q) NaNO₂, HCl, H₂O, 0 °C then urea, H₂SO₄, 50 °C, 15 min, 22%; (r) EtI, K₂CO₃, DMF, 25–45 °C, 30 min, 35%; (s) NH₄COOH, Pd/C, MeOH/H₂O, 60 °C, 30 min, 80%.

compounds which were predicted, using the model outlined above, to be well absorbed. Qualitative *in vitro* studies with liver microsomes⁸ suggested that the main sites of metabolism for compound **2** were oxidation at the benzylic position on the prime side and dealkylation of the non prime side aniline substituent.

Our initial attempts to improve metabolic stability in this series focused on trying to hinder the non prime side aniline based on an early finding that a substitution *ortho* to the hydrogen bond acceptor (HBA) was not detrimental to the activity (compare **6** and **9** with **7**, **8** and **10**, **11**, respectively, Table 3). Moreover, substitution in this position was not detrimental to the selectivity observed over BACE-2 and Cat-D (two aspartic proteases used as our selectivity panel). We hoped to prevent the observed metabolic dealkylation by tying the aniline nitrogen back to the R² substituent in a ring.

The syntheses of the most challenging bicyclic non-prime side chemical intermediates **12–15** which emerged from this endeavour are shown in Scheme 1. The routes described also provided the opportunity to introduce different HBAs at the *meta* position (i.e., R¹):

As shown in Table 4, some 5,6 biaryls inhibitors were slightly more potent than the parent compound **6** (compounds **16–20**) whilst others or 6,6-biaryls were less well tolerated (compounds **23** and **22**, respectively). The latter result (compound **22**) was not easily rationalized and X-ray crystallography failed to provide any significant insights. Superimposition of the structures of compounds **17** and **22** bound to BACE-1⁹ did not reveal any major movements of enzyme residues that could explain the differences in activity observed (Fig. 4).

As shown with representative examples in Table 5, it was also possible to maintain a good level of activity and at the same time potentially minimize the risk of oxidation of the benzylic prime side position either by substitution of this position, by cyclisation or by lowering the electron density of the adjacent ring (compounds **25–27**, respectively).

A further set of compounds which combined the optimal prime and non prime side substituents predicted to afford the appropriate activity and improved metabolic stability were prepared but

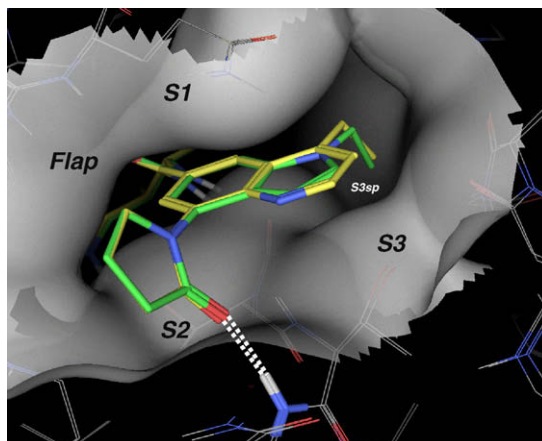
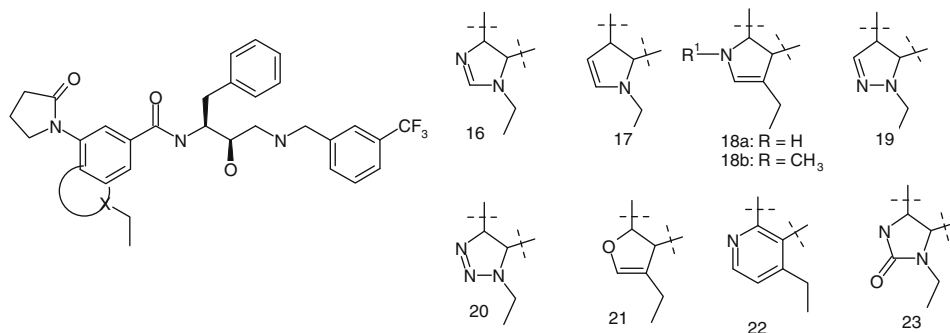


Figure 4. Superimposition on inhibitors **17** (green) and **22** (yellow) bound to BACE-1.

unfortunately without demonstrating a significant improvement in the *in vivo* pharmacokinetics. Compound **28** (Fig. 5), for example, proved to be potent *in vitro* (BACE-1 IC₅₀ = 35 nM) but rapidly cleared *in vivo* (Rat CLb (1 mg/kg iv) = 83 ± 5 mL/min/kg). This result may be explained by either invoking alternative *in vivo* metabolic pathways compared to those observed for compound **2** in microsomes, or by concluding that the changes made to the molecule may have introduced other metabolic liabilities.

Overall, finding a molecule with adequate *in vitro* potency, good absorption and metabolic stability proved difficult to achieve in this series. GSK188909 (compound **2**) appeared to represent one of the best compromises in terms of potency and pharmacokinetics, hence its successful use for target validation, albeit at high oral doses (250 mg/kg po). The discovery of an inhibitor with similar efficacy at acceptable oral doses for clinical studies required the discovery of a novel template which will be the subject of the following publications.

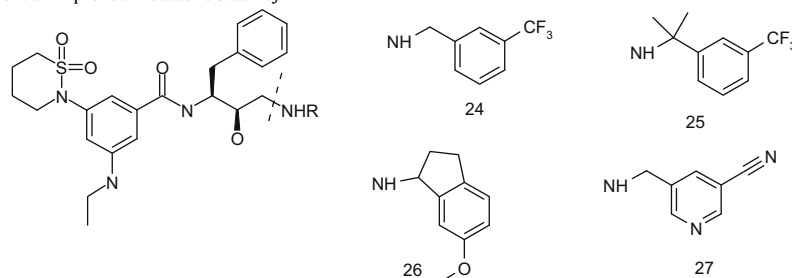
Table 4
Activity and selectivity of selected BACE-1 inhibitors bearing bicyclic non prime side substituents



Compd	BACE-1 IC ₅₀ (μM)	BACE-2 IC ₅₀ (μM)	Cat-D IC ₅₀ (μM)
6	0.049	4.485	6.580
16	0.019	5.75	53.7
17	0.023	8.32	13.49
18a	0.026	5.75	4.07
19	0.028	6.31	14.13
20	0.034	8.91	11.22
18b	0.04	5.13	3.72
21	0.087	12.59	15.14
22	0.21	13.18	14.39
23 ^a	0.42	23.44	23.99

^a Using *m*-MeO benzylic prime side substituent instead of *m*-CF₃.

Table 5
in vitro profile of inhibitors with potential improved metabolic stability



Compd	BACE-1 IC ₅₀ (μM)	BACE-2 IC ₅₀ (μM)	Cat-D IC ₅₀ (μM)
24	0.003	1.41	3.89
25	0.006	0.35	0.60
26^a	0.018	2.95	1.07
27	0.040	7.76	35.48

^a Obtained as a 1:1 mixture of isomers.

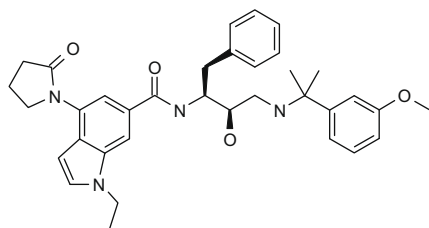


Figure 5. Structure of inhibitor **28**.

References and notes

- Cummings, J. L. *N. Eng. J. Med.* **2004**, *351*, 56.
- (a) Glenner, G. G.; Wong, C. W. *Biochem. Biophys. Res. Commun.* **1984**, *120*, 885; (b) Goedert, M.; Wischik, C. M.; Crowther, R. A.; Walker, J. E.; Klug, A. *Proc. Natl. Acad. Sci. U.S.A.* **1988**, *85*, 4051.
- (a) Hussain, I.; Powell, D.; Howlett, D. R.; Tew, D. G.; Meek, T. D.; Chapman, C.; Gloger, I. S.; Murphy, K. E.; Southan, C. D.; Ryan, D. M.; Smith, T. S.; Simmons, D. L.; Walsh, F. S.; Dingwall, C.; Christie, G. *Mol. Cell Neurosci.* **1999**, *14*, 419; (b) Vassar, R.; Bennett, B. D.; Babu-Khan, S.; Kahn, S.; Mendiaz, E. A.; Denis, P.; Teplow, D. B.; Ross, S.; Amarante, P.; Loeloff, R.; Luo, Y.; Fisher, S.; Fuller, J.; Edenson, S.; Lile, J.; Jarosinski, M. A.; Biere, A. L.; Curran, E.; Burgess, T.; Louis, J. C.; Collins, F.; Treanor, J.; Rogers, G.; Citron, M. *Science* **1999**, *286*, 735; (c) Yan, R.; Bienkowski, M. J.; Shuck, M. E.; Miao, H.; Tory, M. C.; Pauley, A. M.; Brashier, J. R.; Stratman, N. C.; Mathews, W. R.; Buhl, A. E.; Carter, D. B.; Tomasselli, A. G.; Parodi, L. A.; Heinrichson, R. L.; Gurney, M. E. *Nature* **1999**, *402*, 533; (d) Sinha, S.; Anderson, J. P.; Barbour, R.; Basi, G. S.; Caccavello, R.; Davis, D.; Doan, M.; Dovey, H. F.; Frigon, N.; Hong, J.; Jacobson-Croak, K.; Jewett, N.; Keim, P.; Knops, J.; Lieberburg, I.; Power, M.; Tan, H.; Tatsuno, G.; Tung, J.; Schenk, D.; Seubert, P.

- Suomensaaari, S. M.; Wang, S.; Walker, D.; Zhao, J.; McConlogue, L.; John, V. *Nature* **1999**, *402*, 537.
- Review: (a) Durham, T. B.; Shepherd, T. A. *Curr. Opin. Drug Discovery Dev.* **2006**, *9*, 776; (b) Sankaranarayanan, S.; Holahan, M. A.; Colussi, D.; Crouthamel, M.-C.; Devanarayan, V.; Ellis, J.; Espeseth, A.; Gates, A. T.; Graham, S. L.; Gregro, R.; Hazuda, D.; Hochman, J. H.; Holloway, K.; Jin, L.; Kahana, J.; Lai, M.-T.; Lineberger, J.; McGaughey, G.; Moore, K. P.; Nantermet, P.; Pietrak, B.; Price, E. A.; Rajapakse, H.; Stauffer, S.; Steinbeiser, M. A.; Seabrook, G.; Selnick, H. G.; Shi, X.-P.; Stanton, M. G.; Swestock, J.; Tugusheva, K.; Tyler, K. X.; Vacca, J. P.; Wong, J.; Wu, G.; Xu, M.; Cook, J. J.; Simon, A. J. *J. Pharmacol. Exp. Ther.* **2009**, *328*, 131; (c) Charrier, N.; Clarke, B.; Cutler, L.; Demont, E.; Dingwall, C.; Dunsdon, R.; Hawkins, J.; Howes, C.; Hussain, I.; Maile, G.; Matico, R.; Mosley, J.; Naylor, A.; O'Brien, A.; Redshaw, S.; Rowland, P.; Soleil, V.; Smith, K. J.; Sweitzer, S.; Theobald, P.; Vesey, D.; Walter, D. S.; Wayne, G. *J. Med. Chem.* **2008**, *51*, 3313, and references cited herein; (d) Machauer, R.; Laumen, K.; Veenstra, S.; Rondeau, J.-M.; Tintelnnot-Blomley, M.; Betschart, C.; Jatou, A.-L.; Desrayaud, S.; Staufenbiel, M.; Rabe, S.; Paganetti, P.; Neumann, U. *Bioorg. Med. Chem. Lett.* **2009**, *19*, 1366.
 - Beswick, P.; Charrier, N.; Clarke, B.; Demont, E.; Dingwall, C.; Dunsdon, R.; Faller, A.; Gleave, R.; Hawkins, J.; Hussain, I.; Johnson, C. N.; MacPherson, D.; Maile, G.; Milner, P.; Naylor, A.; O'Brien, A.; Redshaw, S.; Riddell, D.; Rowland, P.; Skidmore, J.; Soleil, V.; Smith, K.; Stanway, S.; Stemp, G.; Stuart, A.; Theobald, P.; Vesey, D.; Walter, D. S.; Ward, J.; Wayne, G. *Bioorg. Med. Chem. Lett.* **2008**, *18*, 1022.
 - Hussain, I.; Hawkins, J.; Harisson, D.; Hille, C.; Wayne, G.; Cutler, L.; Buck, T.; Walter, D.; Demont, E.; Howes, C.; Naylor, A.; Jeffrey, P.; Gonzalez, M. I.; Dingwall, C.; Michel, A.; Redshaw, S.; Davis, J. B. *J. Neurochem.* **2007**, *100*, 802.
 - For a discussion around the variability of the transposition of enzyme activity in cellular assays, see Ref. (5).
 - Compound **2** was incubated in liver microsomes and the structures of metabolites were determined via mass-spectroscopy.
 - The PDB deposition codes and refinement details for the BACE-1 complex crystal structures are: **17** (2wez, 1.7 Å resolution, $R = 0.200$, $R_{\text{free}} = 0.223$); **22** (2wf0, 1.6 Å resolution, $R = 0.188$, $R_{\text{free}} = 0.203$).